Double-Peaked Resonance in Harmonic-Free Acoustically Driven Ferromagnetic Resonance

Adi Jung,[1] Dorotea Macri,[1] Samuel Margueron,[2] Ausrine Bartasyte,[2] and Sayeef Salahuddin[1]
[1)] *Department of Electrical Engineering and Computer Sciences, University of California, Berkeley, CA-94720, USA*
[2)] *FEMTO-ST Institute, University of Bourgogne Franche-Comté, 26 rue de l'Epitaphe, Besancon 25030, France*

(Dated: March 30, 2021)

Resonant interaction between surface acoustic waves (SAWs) and ferromagnetic thin films, a phenomenon known as acoustically driven ferromagnetic resonance (ADFMR), provides a way to control magnetic resonance with purely voltage excitation. However, devices have historically been operated at harmonic frequencies, leading to large insertion losses. In this work, we demonstrate harmonic-free response of ADFMR devices where the strain reaches very high values, comparable to the saturation magnetostriction of the magnetic element. The acoustic energy transfer is highly efficient and reaches almost 99.9%. Furthermore, we report the presence of multiple absorption maxima across the range of applied magnetic fields, a property not previously observed in the literature.

The phenomenon of acoustically driven ferromagnetic resonance (ADFMR) has gained attention in recent years in a number of novel application spaces. The theoretical framework for ADFMR was initially developed by Kittel in 1956, who predicted a highly efficient conversion of energy from acoustic phonons into spin wave modes of a ferromagnetic film.[1] Typical experiments by Kittel's contemporaries studied the phenomenon by evaporating a magnetic film onto a quartz rod, driving the film into ferromagnetic resonance, and measuring the amplitude of the generated acoustic wave via a microwave cavity.[2,3] In recent years, photolithography and nanofabrication techniques have advanced to the point where GHz surface acoustic waves (SAWs) can be transmitted and received via interdigitated transducers (IDTs).[4] This has enabled a variety of novel studies of magnetoelasticity in thin films, including film characterization[5,6] and interactions with quantum defects.[7]

In a typical modern ADFMR study, SAWs are generated on a piezoelectric substrate and propagate through a ferromagnetic thin film under an applied magnetic bias field. This bias field is varied in amplitude and direction, and the resulting change in transmitted acoustic power is measured. In the majority of prior work, studies of ADFMR at GHz frequencies have relied on IDTs driven at high harmonics to produce the surface acoustic waves.[5,6,8,9] As a result, these IDTs have suffered from high insertion losses, in turn severely limiting the amount of power delivered to the magnetic thin film. In this paper, we report a study of ADFMR driven by low-loss IDTs operated at their fundamental frequency. The acoustic drive is harmonic-free and of a higher amplitude than in prior reports, and is now of comparable amplitude to the saturation magnetostriction of Ni.[10] Furthermore, a qualitative difference in the absorption line-shape is observed as compared to prior work.

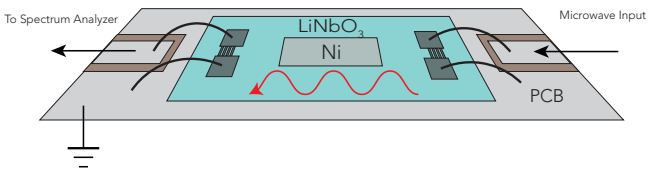

Figure 1. Diagram of the device and PCB mount. Transmitter and receiver IDTs are wirebonded to the PCB waveguide by Al wire. The acoustic opening of the IDTs along the $LiNbO_3$ is 100μm, and the IDT input impedance is designed to be 50Ωat the center frequency of 2.6 GHz. IDTs pairs were separated by a distance of 2mm, and the Ni pad was 600μm long and 150μm wide.

ADFMR devices in this study were fabricated on a 128°YX-cut $LiNbO_3$ substrate. The IDT pairs were patterned via lift-off of an 80nm evaporated Al film, and were designed to operate at a fundamental frequency of 2.6 GHz, with an acoustic opening of 100 μm. Following IDT fabrication, 20nm thick Ni thin films were deposited between IDT pairs by e-beam evaporation, and patterned via lift-off. In order to verify that the Ni deposition process had no impact on IDT performance, devices were fabricated both with and without Ni pads. The resulting Ni pad was of width 150 μm and length in the SAW propagation direction of 600 μm. A diagram of the device is provided in Fig 1.

Following microfabrication, the IDTs were wirebonded to 50Ω coplanar waveguides on a custom built PCB. The total transmission loss in the PCB alone was approximately 3 dB, due to impedance mismatch caused by the self-inductance of the wirebonds. To quantify the total transmission loss of the combined PCB-IDT system, 2-port S-parameters for control IDT pairs with no Ni layer between them were measured using a vector network analyzer. The acoustic transmission was time-gated, isolating the signal from spurious signals due to electromagnetic transmission and SAW triple-transit signals, similar to the methodology detailed in prior SAW-driven ADFMR measurements.[9] The transmitted signal consisted of an electromagnetic pulse, the primary acoustic pulse, and a number of smaller pulses related to triple-transit and spurious reflections off of adjacent IDTs. To guarantee that these spurious reflections did not overlap with the primary pulse in the time domain, potentially compromising the time-gating process, IDT transmission was measured with adjacent IDTs coated in photoresist. Transmitted power was found to be unchanged relative to measurements without the photoresist, indicating that all spurious reflections due to nearby transducers

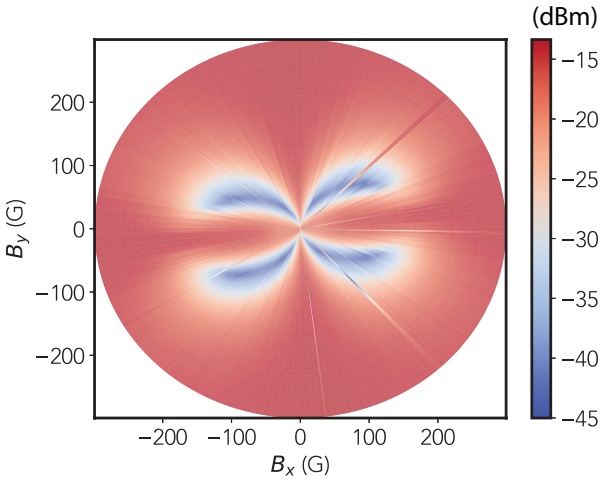

Figure 2. Angular field sweep of 20nm thick Ni film at an applied input power of 0 dBm. The color bar indicates the transmitted power in dBm, where the X direction represents the propagation direction of the SAW.

were successfully filtered out by the time-gating process. Further details of the time-gating methodology may be found in the supplemental material. Finally, following characterization and time-gating, the IDT pairs without a Ni pad were found to have an insertion loss of approximately 17 dB.

After loss characterization in the PCB-IDT system, devices with a deposited Ni film were placed on a rotational stage between coils of an electromagnet, and SAW transmission was characterized under a sweep of DC magnetic bias field and direction. To reduce measurement times, the vector network analyzer was replaced by a pulsed RF function generator at the input port, and the output port was fed into a spectrum analyzer. The function generator was configured to output 2.6 GHz pulses with a pulse width of 700 ns, and the spectrum analyzer measurement was synchronized to these pulses, implementing an equivalent time-gating process in the test hardware.

The applied DC magnetic field was swept through 360°and through field magnitudes of 0 to 300 G at varying microwave input powers. The absorption characteristic of the device at an input power of 0 dBm is provided in Fig 2. The 4-lobed absorption characteristic of ADFMR was observed, and the fractional power absorption on resonance remained constant over a 2 order of magnitude increase in input power.

To illustrate key details of the SAW absorption, two linecuts of the absorption data are plotted: along curves of peak absorption, and along field sweeps at angles of maximum absorption. Curves of peak absorption for each absorption lobe are plotted in Fig 3a at various input powers. The angle of maximum power absorption at each given field value is determined, and the value of maximum absorption is plotted as a function of field value. The trajectories being followed in Fig 3a are overlaid over the field-swept absorption data in Fig 3b. Two absorption peaks within each lobe can be clearly seen, in contrast to prior measurements of ADFMR absorption

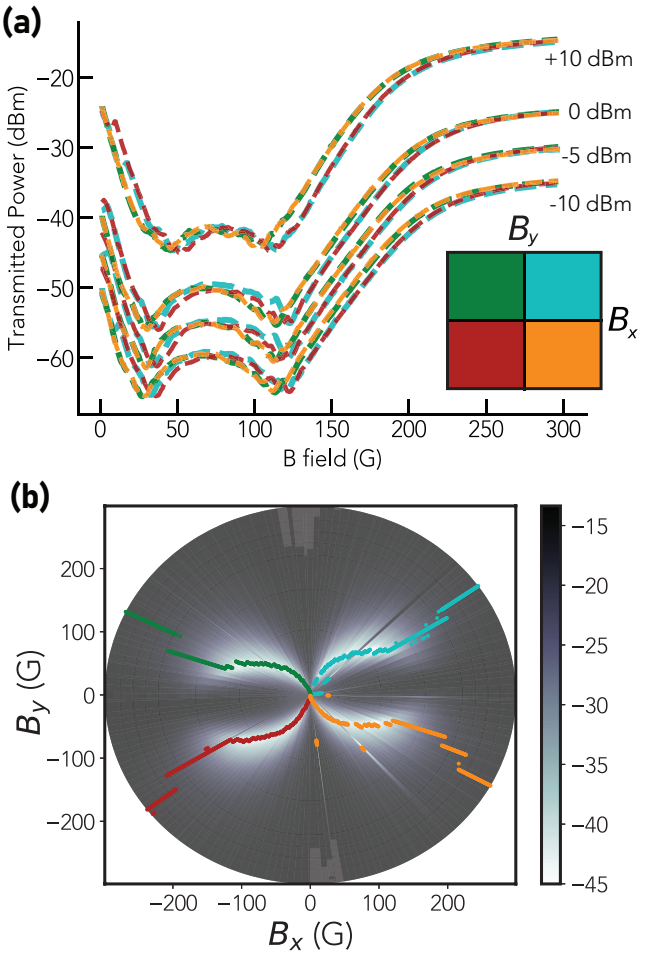

Figure 3. (a) Curves of peak absorption are plotted for each of the 4 lobes (color-coded) for various input powers. Two points of maximum absorption are clearly visible within each lobe. Small qualitative differences between the +10 dBm power level and the others are due to the use of different internal circuitry within the spectrum analyzer. The absorption curves deviate from each other slightly for lobes rotated by 90°; this is attributed to the presence of small shear strain components in the Rayleigh wave. (b) The trajectory of the linecut in (a) is overlaid over the field sweep data for the 0 dBm input power level.

in $LiNbO_3$/Ni stacks.[6] The slight variation in resonance peak depth and position at +10 dBm compared to the lower applied powers is attributed to circuit switching within the spectrum analyzer, which results in a higher noise floor at that power level.

For the field sweeps at angles of maximum absorption, the two angles at which absorption peaks occur within each lobe are determined, and power absorption is plotted vs. applied field for these angles in Fig 4. While two separate maxima are observed over the full range of applied DC magnetic fields and angles, the absorption line-shapes remain consistent with those previously reported, and are qualitatively similar to those of traditional FMR measurements.

Furthermore, we note that while nonreciprocal transmission of SAWs through piezoelectric-ferromagnet multilayers

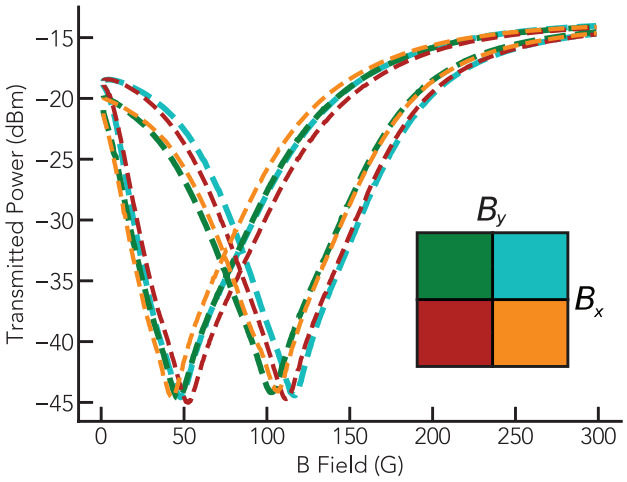

Figure 4. Field sweeps along angles of maximum absorption are plotted for each lobe (color-coded) here. The fields of maximum absorption are ≈ 50 G and ≈ 110 G for each lobe, and the lineshapes remain approximately Lorentzian, consistent with prior studies on ADFMR.

has been reported in a number of ADFMR devices,[11,6,12], we observe no such nonreciprocal transmission under a magnetic field rotation of 180 degrees. The slight variation in transmission in perpendicular lobes can be explained by small shear wave-driven magnetoelastic fields in conjunction with the dominant longitudinal contribution within the Rayleigh wave.[9]

The SAW strain amplitude within the Ni film was estimated following the methodology of Warner et.al.[13] In this procedure, displacement and electric potential in Rayleigh waves are represented as sums of 4 partial wave solutions, taking on the form:

$$u_i = \sum_{r=1}^{4} \beta_i^{(r)} e^{-\alpha^{(r)} kz} e^{i(\omega t - kx)} \tag{1a}$$

$$\phi = \sum_{r=1}^{4} \beta_4^{(r)} e^{-\alpha^{(r)} kz} e^{i(\omega t - kx)} \tag{1b}$$

where u_i represents the displacement vector, and ϕ represents the electric potential. The wave parameters k, α, and β_i are solved for each partial wave according to surface wave boundary conditions and the piezoelectric equations of motion and constitutive equations. The details of this process may be found in the supplemental material.

In order to normalize the wave amplitudes to the experimentally delivered power, two critical assumptions are made. Firstly, the SAW amplitude within the ferromagnet is approximated to be equal to the strain at the surface of an infinitesimal conductive layer above $LiNbO_3$. Secondly, the losses are assumed to be symmetric across the device, indicating that delivered acoustic power is reduced by half of the dB value of insertion loss. The resulting approximations of longitudinal and shear strain components are provided in Table I. This indicates that strains in these devices are indeed comparable

Table I. Estimated strain components for acoustic waves at varying applied RF power.

Input Power (dBm)	ε_{xx} (um/um)	ε_{xy} (um/um)	ε_{xz} (um/um)
+10	2e-4	1e-5	1e-6
0	6e-5	4e-6	3e-7
-5	3e-5	2e-6	2e-7
-10	2e-5	1e-6	1e-7

to or in excess of the saturation magnetostriction of polycrystalline Ni thin films, reported in literature to be $-3.8 * 10^{-5}$.[10]

In conclusion, efficiently excited ADFMR devices operate robustly at higher strain values than previously shown, and the linear response with respect to input power is maintained over a wide range of power levels typical of RF devices. As a result, signal-to-noise ratio in virtually all applications can be improved at a particular input power level. Of particular interest is the potential application case of ADFMR-coupled quantum defects, as this interaction has already been shown to be highly efficient in prior work, and may be further improved by minimized system losses. Furthermore, the presence of multiple SAW absorption maxima introduces a new tool for engineering the magnetoelastic response of ADFMR devices. This may enable novel applications in the growing field of non-reciprocal magnetoelastic SAW devices.

ACKNOWLEDGMENTS

This work was supported in part by the NSF TANMS center. This work has been supported by the EIPHI Graduate School contract ANR 17 EURE 0002 and by the French RENATECH network and its FEMTO-ST technological facility. The authors would also like to acknowledge many fruitful discussions with Dr. Dominic Labanowski.

REFERENCES

[1] C. Kittel, "Interaction of Spin Waves and Ultrasonic Waves in Ferromagnetic Crystals," Physical Review **110**, 836–841 (1958).
[2] H. Bömmel and K. Dransfeld, "Excitation of Hypersonic Waves by Ferromagnetic Resonance," Physical Review Letters **3**, 83–84 (1959), publisher: American Physical Society.
[3] M. Pomerantz, "Excitation of Spin-Wave Resonance by Microwave Phonons," Physical Review Letters **7**, 312–313 (1961), publisher: American Physical Society.
[4] A. Coon, "SAW filters and competitive technologies: a comparative review," in *IEEE 1991 Ultrasonics Symposium,* (1991) pp. 155–160 vol.1.
[5] D. Labanowski, A. Jung, and S. Salahuddin, "Power absorption in acoustically driven ferromagnetic resonance," Applied Physics Letters **108**, 022905 (2016), publisher: American Institute of Physics.
[6] R. Sasaki, Y. Nii, Y. Iguchi, and Y. Onose, "Nonreciprocal propagation of surface acoustic wave in Ni/$LiNbO_3$," Physical Review B **95**, 020407 (2017), publisher: American Physical Society.
[7] D. Labanowski, V. P. Bhallamudi, Q. Guo, C. M. Purser, B. A. McCullian, P. C. Hammel, and S. Salahuddin, "Voltage-driven, local, and efficient excitation of nitrogen-vacancy centers in diamond," Science Advances **4** (2018), 10.1126/sciadv.aat6574, publisher: American Association for the Advancement of Science Section: Research Article.

[8]J. Puebla, M. Xu, B. Rana, K. Yamamoto, S. Maekawa, and Y. Otani, "Acoustic ferromagnetic resonance and spin pumping induced by surface acoustic waves," Journal of Physics D: Applied Physics **53**, 264002 (2020), publisher: IOP Publishing.

[9]M. Pernpeintner, *Magnon-Phonon Coupling in Ferromagnetic Thin Films*, Ph.D. thesis, Walther-Meissner-Institute for Low Temperature Research (2012).

[10]E. Klokholm and J. Aboaf, "The saturation magnetostriction of thin polycrystalline films of iron, cobalt, and nickel," Journal of Applied Physics **53**, 2661–2663 (1982), publisher: American Institute of Physics.

[11]M. Küß, M. Heigl, L. Flacke, A. Hörner, M. Weiler, M. Albrecht, and A. Wixforth, "Nonreciprocal Dzyaloshinskii-Moriya magnetoacoustic waves," arXiv:2004.03535 [cond-mat] (2020), arXiv: 2004.03535.

[12]P. J. Shah, D. A. Bas, I. Lisenkov, A. Matyushov, N. Sun, and M. R. Page, "Giant Nonreciprocity of Surface Acoustic Waves enabled by the Magnetoelastic Interaction," arXiv:2004.14190 [cond-mat, physics:physics] (2020), arXiv: 2004.14190.

[13]A. W. Warner, M. Onoe, and G. A. Coquin, "Determination of Elastic and Piezoelectric Constants for Crystals in Class (3m)," The Journal of the Acoustical Society of America **42**, 1223–1231 (1967), publisher: Acoustical Society of America.

[14]A.J. Slobondik, E. Conway, and R. Delmonico, *Microwave Acoustics Handbook: Surface wave velocities.*, Vol. 1A (Air force Cambridge research laboratories, 1973).

[15]D. A. Bas, P. J. Shah, M. E. McConney, and M. R. Page, "Optimization of acoustically-driven ferromagnetic resonance devices," Journal of Applied Physics **126**, 114501 (2019), publisher: AIP Publishing LLCAIP Publishing.

[16]D. Labanowski, A. Jung, and S. Salahuddin, "Effect of magnetoelastic film thickness on power absorption in acoustically driven ferromagnetic resonance," Applied Physics Letters **111**, 102904 (2017), publisher: American Institute of Physics.

[17]D. A. Bas, P. J. Shah, A. Matyushov, M. Popov, V. Schell, R. C. Budhani, G. Srinivasan, E. Quandt, N. Sun, and M. R. Page, "Acoustically Driven Ferromagnetic Resonance in Diverse Ferromagnetic Thin Films," IEEE Transactions on Magnetics , 1–1 (2020).

[18]M. Weiler, L. Dreher, C. Heeg, H. Huebl, R. Gross, M. S. Brandt, and S. T. B. Goennenwein, "Elastically Driven Ferromagnetic Resonance in Nickel Thin Films," Physical Review Letters **106**, 117601 (2011), publisher: American Physical Society.

[19]L. Thevenard, C. Gourdon, J. Y. Prieur, H. J. von Bardeleben, S. Vincent, L. Becerra, L. Largeau, and J.-Y. Duquesne, "Surface-acoustic-wave-driven ferromagnetic resonance in (Ga,Mn)(As,P) epilayers," Physical Review B **90**, 094401 (2014), publisher: American Physical Society.

[20]D. Labanowski, *Acoustically Driven Ferromagnetic Resonance for Device Applications*, Ph.D. thesis, EECS Department, University of California, Berkeley (2019).